



## Defluoridation of water using synthesized Zr(IV) encapsulated silica gel/chitosan biocomposite: Adsorption isotherms and kinetic studies

Subbaiah Muthu Prabhu, Sankaran Meenakshi\*

Department of Chemistry, The Gandhigram Rural Institute - Deemed University, Gandhigram, Dindigul 624 302, Tamil Nadu, India

Tel. +91 451 2452371; Fax: +91 451 2454466; email: [drs\\_meena@rediffmail.com](mailto:drs_meena@rediffmail.com)

Received 12 August 2013; Accepted 26 November 2013

---

### ABSTRACT

Fluoride contamination of groundwater, both anthropogenic and natural, is a major problem worldwide. This investigation reports the synthesis of a new adsorbent material, Zr(IV) encapsulated silica gel/chitosan (Zr-SGCS) composite. The silica gel/chitosan (SGCS) composite, which has a desirable defluoridation capacity (DC) of 3402 mgF<sup>-</sup>/kg, has been further chemically modified by incorporating Zr<sup>4+</sup> ion into SGCS composite and its DC was found to be 4,530 mgF<sup>-</sup>/kg. The suitability of Zr-SGCS composite for the removal of fluoride was assessed by batch method and optimized various parameters viz., contact time, dosage, pH, co-ions, and temperature that influence the sorption. The fluoride sorption was explained using Freundlich, Langmuir, and D-R isotherms. The Freundlich isotherm equation described the fluoride sorption equilibrium well at 303, 313, and 323 K and the thermodynamic parameters such as  $\Delta G^\circ$ ,  $\Delta H^\circ$ , and  $\Delta S^\circ$  indicated that the nature of fluoride sorption was spontaneous and endothermic. The surface morphology of composites before and after fluoride sorption was observed using scanning electron microscopy. Fourier transform infrared spectroscopy was taken to confirm the respective functional groups present in the sorbents.

*Keywords:* Chitosan; Zirconium; Silica gel; Fluoride; Sorption isotherms; Kinetic studies

---

### 1. Introduction

Water is one of the major elements essential for sustenance of all forms of life and is available in abundance in nature covering approximately three-fourths of the surface of the earth. Fluoride (F<sup>-</sup>) contamination in groundwater has been recognized as one of the serious problems worldwide [1]. Fluoride in drinking

water resembles a two-edged sword depending on its concentration and the total amount ingested. Fluoride ion, within the tolerance limit (<1.5 mg/L) is essential for the formation of caries resistant dental enamel and for the normal mineralization in hard tissues. Because of the beneficial role of fluoride, WHO included fluoride in its list as one of the trace elements essential for human health [2]. BIS (Beuro of Indian Standards) standards, for fluoride in drinking water, are 1.0 mg/L as permissible and 1.5 mg/L as maximum permissible level [3]. One of the most important

---

\*Corresponding author.

preventive measures of fluorosis is provision of drinking water containing fluoride within the tolerance limits. A number of methods have been suggested for the defluoridation of water namely chemical precipitation, ion exchange, adsorption, nanofiltration, reverse osmosis, electrolysis, and Donnan Dialysis [4–10]. Among the methods reported, adsorption seems to be the most attractive, promising, and selective technique for fluoride removal [11–14].

Chitosan produced from N-deacetylation of chitin is normally recognized as a sorbent for removing cations and extensively studied for heavy metal removal [15]. Only a few reports are available about its capacity to remove fluoride [16–18]. In sorption process, chitosan is often used in the form of flakes or powder which is less stable and causes a significant pressure drop which would affect filtration during field applications [19]. The defluoridation capacity (DC) of the raw chitosan was found to be minimum. Due to the peculiar features like nontoxicity, bi-functionality, high biocompatibility, biodegradability, and commercial availability, chitosan has been one of the most largely studied natural biopolymeric materials [20–22]. Currently, chitosan-based organic-inorganic hybrid composites take an increasing importance. Hence, chitosan has been selected as the organic polymeric matrix to prepare the hybrid sorbents with the selected inorganic materials for the present study. Silica supported polymeric hybrid materials using chitosan, cellulose, polystyrene, etc. were used in the heavy metal removal, biosensor, catalyst, chromatography, etc. [23–30]. Rajiv Gandhi and Meenakshi [31] have extensively studied the application of silica gel/chitosan (SGCS) hybrid composite for copper and lead removal.

Zirconium possesses higher affinity towards fluoride; a number of publications also reported the use of zirconium based material as sensor in automated analysis of fluoride in water [32,33]. Hence, in this communication, the fluoride removal studies using Zr(IV) encapsulated silica gel/chitosan composite (Zr-SGCS) has been reported. The effects of pH, shaking time, and adsorbent dosage on the removal of fluoride were investigated in this study. A possible mechanism of fluoride removal by the Zr-SGCS composite was also suggested.

## 2. Experimental section

### 2.1. Materials

The chitosan flakes with average molecular weight of 400 kDa and 85% degree of deacetylation was obtained from Pelican Biotech and Chemicals Labs,

Kerala (India). Silica gel (SG) GLR TLC grade was purchased from S.D. Fine-Chem limited, Mumbai.  $ZrOCl_2 \cdot 8H_2O$ , glacial acetic acid, glutaraldehyde was obtained from Merck, Mumbai and all other chemicals used were of analytical grade.

### 2.2. Synthesis of SGCS composite

SG was heated at 110°C for 1 h to activate the surface. The chitosan was dissolved in 2% acetic acid solution and stirred for 1 h and then the required amount of glutaraldehyde was added. The mixture was stirred for 2 h and soaked in an ultrasonic bath for 30 min and then the activated SG was added. The wet gel was allowed to evaporate at room temperature to complete cross-linking reaction and gelation. The dry product obtained was washed thoroughly with distilled water and dried in oven at 40°C [24,31]. Finally, the dried SGCS hybrid composite was sieved to uniform size and used for fluoride sorption studies.

### 2.3. Synthesis of Zr-SGCS composite

SG was heated at 110°C for 1 h to activate the surface. The chitosan was dissolved in 2% acetic acid solution and 5 g of  $ZrOCl_2 \cdot 8H_2O$  was added and stirred for 1 h and then the required amount of glutaraldehyde was added. The mixture was stirred for 2 h and soaked in an ultrasonic bath for 30 min before the activated SG was added. The wet gel was allowed to evaporate at room temperature to complete cross-linking reaction and gelation. The dry product obtained was washed thoroughly with distilled water to neutral pH and dried in oven at 40°C [24,31]. Finally, the dried Zr-SGCS hybrid composite was sieved to uniform size and used for fluoride sorption studies.

### 2.4. Physical characterization measurements

Expandable ion Analyzer EA 940 with Orion ion plus (9609) fluoride electrode (Thermo Electron Corporation, USA) was used for fluoride measurement. The pH measurement was done by a Cyber Scan 510 pH meter (Oakton Instruments, USA). A temperature controlled orbital shaker (Remi Instruments Ltd., Mumbai, India) was used for agitation of the samples in batch studies. A high precision electrical balance (Shimadzu, AY 220 model) was used for weight measurement. All other water quality parameters were analyzed by using standard methods [34,35].

Fourier transform infrared spectroscopy (FTIR) spectra of the composite were recorded with JASCO-460 plus model using KBr pellets prepared by

mixing composite with KBr. The KBr pellet technique was used and the spectra data was recorded from 4,000 to 400  $\text{cm}^{-1}$  with a resolution of 4  $\text{cm}^{-1}$ . The results of FTIR were used to confirm the functional groups present in the composite.

The surface morphology of the composite was visualized by scanning electron microscopy (SEM) with Vega3 Tescan model. The SEM enables the direct observation of the surface microstructures of the fresh and fluoride-sorbed composite. Elemental spectra of the composite were obtained using an energy dispersive X-ray analyzer (EDAX-Bruker Nano GMBH, Germany) during SEM observations which allows a qualitative detection and localization of elements in the composite. The surface area of the composite was measured using Micromeritics–Tristar 3000 model.

Computations were made using Microcal Origin (Version 6.0) software. The goodness of fit was discussed using regression correlation coefficient ( $r$ ), chi-square analysis ( $\chi^2$ ), and standard deviation (SD). All the experiments were conducted in triplicate.

### 2.5. Adsorption studies

Batch experiment was carried out by adding fixed amount of the adsorbent material to 50 mL of test solution in a conical flask which was kept in a shaker for a fixed time. Stock solution of sodium fluoride containing 100 mg/L was prepared and this was used for fluoride sorption experiments after proper dilution. Initial fluoride concentration was maintained as 10 mg/L for all the experiments and the mixture was agitated at 200 rpm in a mechanical shaker. The solution was then filtered and the residual fluoride concentration was measured. The kinetic and thermodynamic parameters of the adsorption were established by conducting the experiments at 303, 313, and 323 K in a temperature controlled mechanical shaker.

## 3. Results and discussion

### 3.1. Contact time

The DC of Zr-SGCS, SGCS, and Zr-CS composite can vary with the period of contact with the sorbate solution. The sorption of fluoride has been investigated as a function of time in the range of 10–70 min with 10 mg/L as initial fluoride concentration at room temperature and shown in Fig. 1. From the graph, it is evident that the DC of both the sorbents increases with increasing time and finally reaches saturation at 60 min. Hence, for further experiments, the contact time was fixed as 60 min. The DCs of Zr-SGCS, SGCS, and

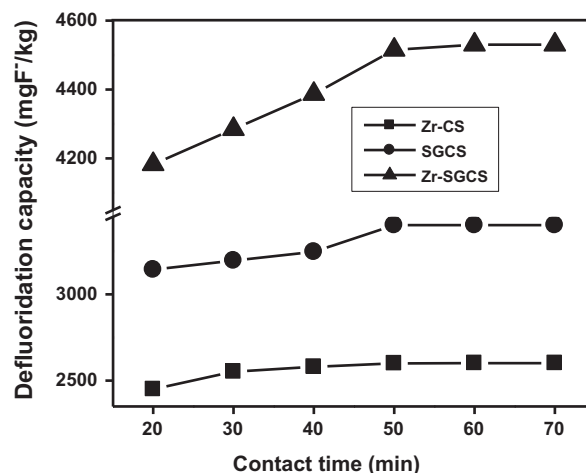


Fig. 1. Contact time on DC of Zr-CS, SGCS, and Zr-SGCS composite.

Zr-CS composite were 4,530, 3,402 and 2,601  $\text{mgF}^{-}/\text{kg}$ , respectively. Zr-CS composite showed lower DC than SGCS and Zr-SGCS composite. Hence, further studies were limited to SGCS and Zr-SGCS composites.

### 3.2. pH

The effect of pH on the DCs of SGCS and Zr-SGCS composite was carried out at five different initial pH levels, namely, 3, 5, 7, 9, and 11 by keeping other parameters as constant as follows: contact time, 60 min; dosage, 0.1 g; initial fluoride, 10 mg/L; and temperature, 303 K. The pH of the working solution was controlled by adding HCl/NaOH solution. The maximum DC was observed as 4,490  $\text{mgF}^{-}/\text{kg}$  at pH 7 and a minimum of 4,133  $\text{mgF}^{-}/\text{kg}$  DC at pH 11 for Zr-SGCS

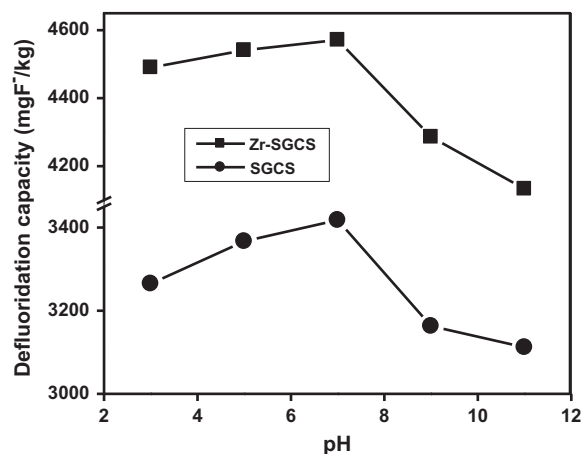


Fig. 2. pH on DC of the Zr-SGCS and SGCS composite.

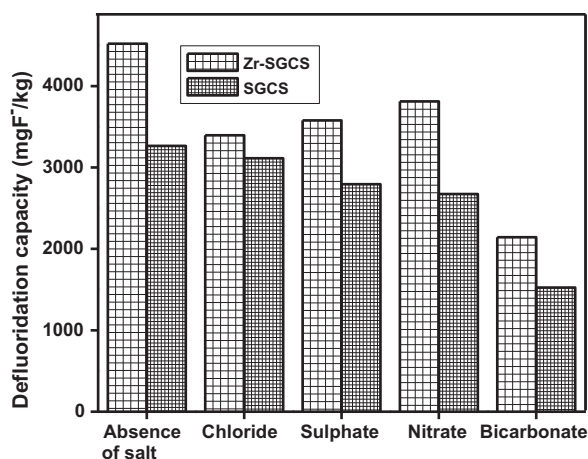


Fig. 3. Effect of coexisting anions on DC of the Zr-SGCS and SGCS composite.

composite and maximum DC was observed as 3,402 mgF<sup>-</sup>/kg at pH 7 and minimum of 3,150 mgF<sup>-</sup>/kg at pH 11 for SGCS composite. It is clear that the fluoride removal was slightly altered at higher pH of the medium for both the composites (Fig. 2). Hence, pH 7 was optimized for further experiments as the DC was higher at this pH of the medium.

### 3.3. Co-existing anions

The fluoride-contaminated water may contain several other anions which may compete with the sorption of fluoride. The adsorption studies were carried out in the presence of 20–200 mg/L salt solutions of chloride, nitrate, sulfate, and bicarbonate independently at an initial fluoride concentration of 10 mg/L. From Fig. 3, it is evident that the overall DC of the composite was slightly decreased in the presence of Cl<sup>-</sup>, SO<sub>4</sub><sup>2-</sup>, and NO<sub>3</sub><sup>-</sup> ions, but the presence of HCO<sub>3</sub><sup>-</sup> ions significantly reduced for both Zr-SGCS and SGCS composites. This may be due to the competition of bicarbonate ions with fluoride ions in the sorption process.

Table 1  
Characteristics of Zr-SGCS composite

Constituents	Zr-SGCS composite
Inorganic material	SG, Zirconium
Organic matrix	Chitosan cross-linked with glutaraldehyde
Particle size (nm)	244
Density (g/cm <sup>3</sup> )	0.810
BET surface area (m <sup>2</sup> /g)	6.035

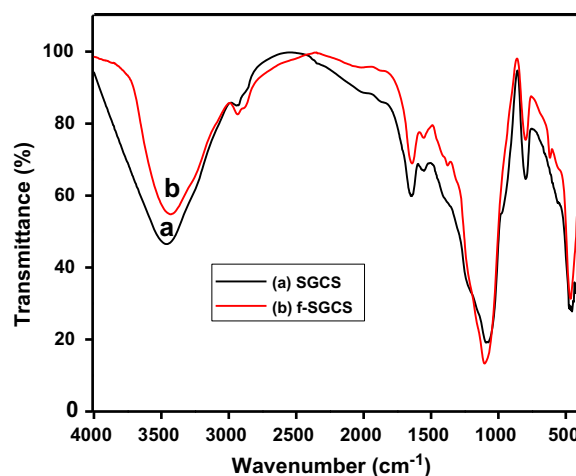


Fig. 4. FTIR spectra of (a) SGCS and (b) f-SGCS composite.

### 3.4. Characterization of sorbent

The Zr-SGCS composite was characterized by measuring the parameters viz. particle size, density, BET surface area, and are presented in Table 1. Fig. 4 shows the FTIR spectra of SGCS composite before and after sorption of fluoride. The major bands for the chitosan in the SGCS composite can be assigned as follows: 3,461 cm<sup>-1</sup> (OH and NH<sub>2</sub> stretching vibrations), 2,942 cm<sup>-1</sup> (CH stretching vibration in CH and CH<sub>2</sub>), 1,643 cm<sup>-1</sup> (NH<sub>2</sub> bending vibration), 1,076 cm<sup>-1</sup> (CO stretching vibration in CONH), and the bands at 3,461 cm<sup>-1</sup> (stretching vibration in surface hydroxyl), 1,091 cm<sup>-1</sup> (stretching vibration of Si-O), and 476 cm<sup>-1</sup> (twisting vibration of Si-O-Si) are assigned to the SG in the SGCS composite [31].

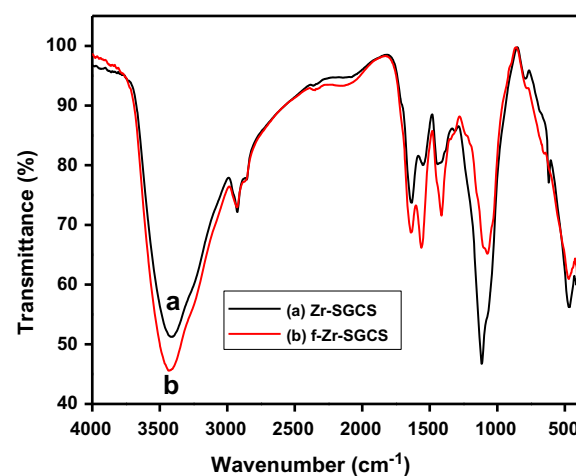


Fig. 5. FTIR spectra of (a) Zr-SGCS and (b) f-Zr-SGCS composite.

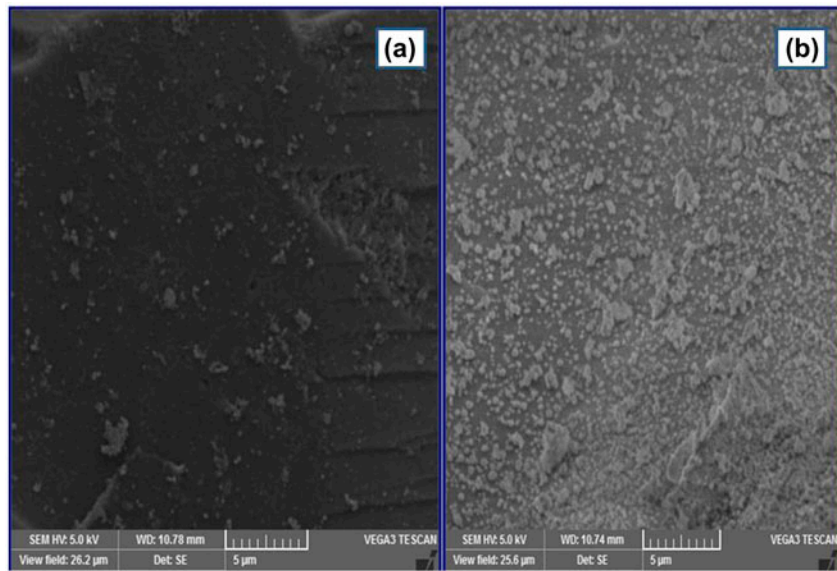


Fig. 6. SEM micrographs of (a) SGCS and (b) f-SGCS composite.

Fig. 5 shows the FTIR spectra of Zr-SGCS and fluoride sorbed Zr-SGCS (f-Zr-SGCS) composite. The broad, strong band in the  $3,415\text{ cm}^{-1}$  range may be due to the  $-\text{OH}$  bending vibrations, which show the presence of surface hydroxyl groups and physically absorbed water [36–39]. The sharp band at  $2,925$  and  $1,633\text{ cm}^{-1}$  confirms the presence of  $-\text{CH}$  stretching vibrations and  $-\text{NH}_2$  bending vibrations in the chitosan. The peak at  $1,440\text{ cm}^{-1}$  corresponds to  $\text{C}-\text{N}$  stretching vibrations present in the chitosan. A band in the region of  $980\text{--}1,200\text{ cm}^{-1}$  indicates for  $\text{Zr}-\text{O}-\text{Si}$  stretching vibration [40–42]. A band at  $790$  and  $465\text{ cm}^{-1}$  indicates the symmetric stretching and

bending vibrations of  $\text{Si}-\text{O}-\text{Si}$  bond, respectively [31]. The peak at  $618\text{ cm}^{-1}$  is assigned for  $\text{Zr}-\text{O}-\text{C}$  stretching vibration [43]. Fig. 5 shows a slight broadening at  $3,440\text{ cm}^{-1}$  and shifting of other bands in the f-Zr-SGCS composite and this may be due to electrostatic adsorption between the sorbent and the fluoride [44,45].

### 3.5. Morphological analysis by SEM

Surface morphology is an important factor in adsorbent-adsorbate interactions. The SEM pictures of SGCS composite, and Zr-SGCS composite before and after treatment with fluoride are shown in Figs. 6(a), (b) and

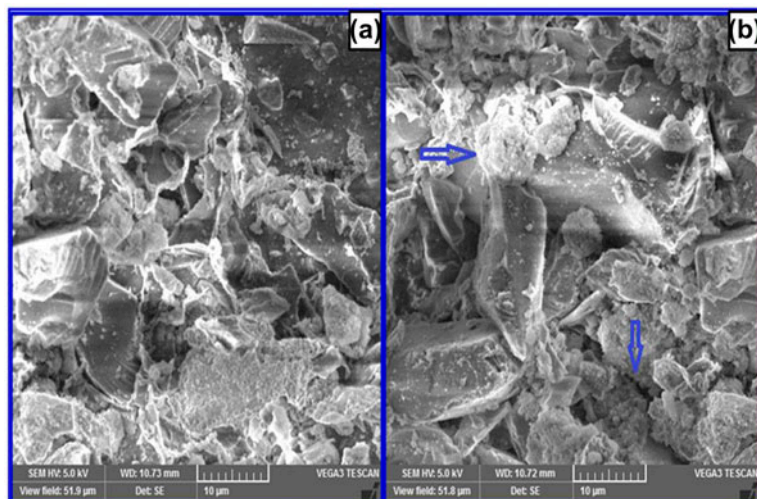


Fig. 7. SEM micrographs of (a) Zr-SGCS and (b) f-Zr-SGCS composite.

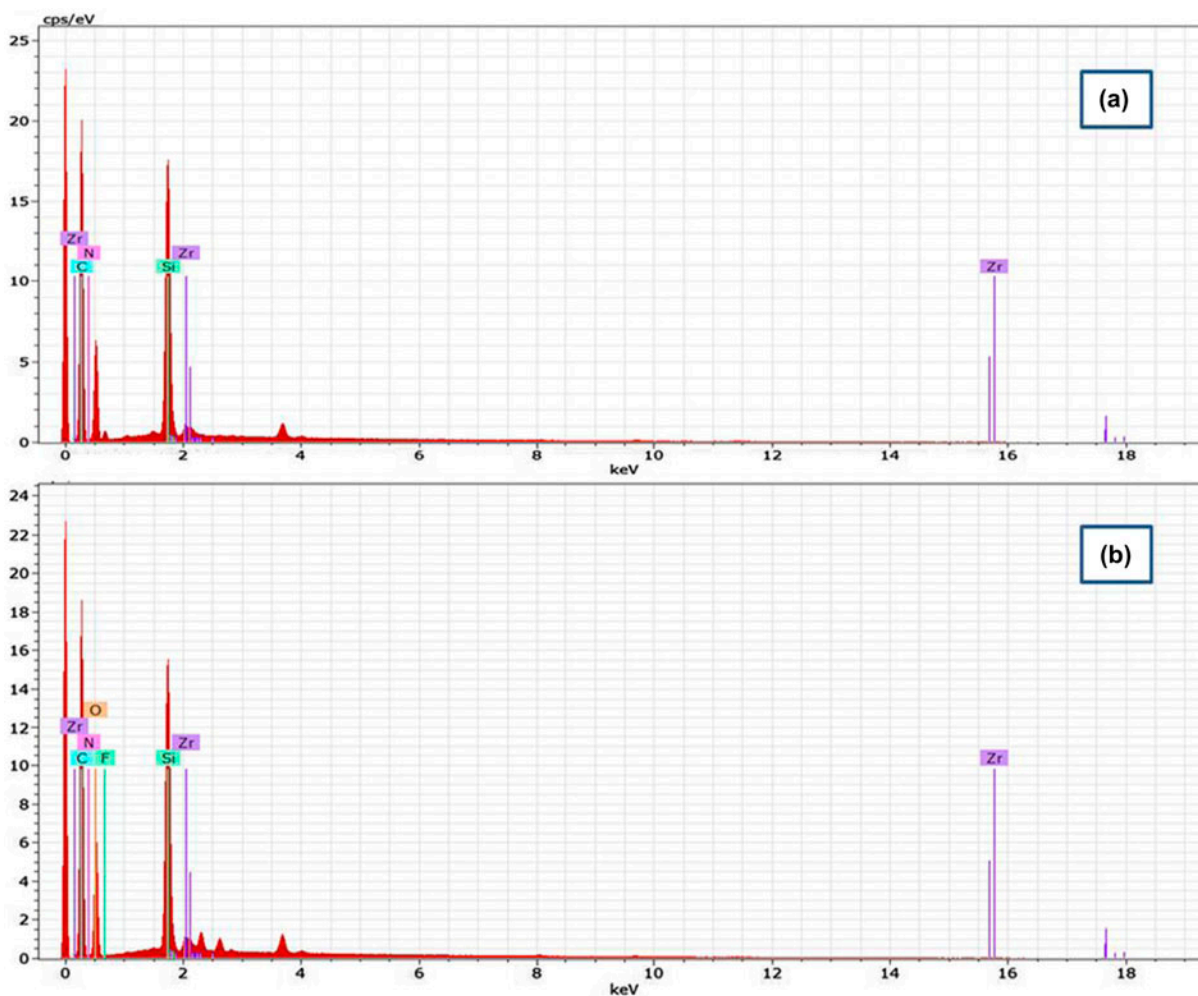


Fig. 8. EDAX spectra of (a) Zr-SGCS and (b) f-Zr-SGCS composite.

7(a), (b). The changes in the surface morphology of both composites before and after fluoride treatment indicate the fluoride sorption on the respective composites. This is also further supported by EDAX analysis. The EDAX spectrum of Zr-SGCS composite confirms the elements present in it and is shown in Fig. 8(a). The presence of a fluoride peak in the EDAX spectra of fluoride-sorbed Zr-SGCS composite confirms the fluoride sorption onto Zr-SGCS composite which is shown in Fig. 8(b).

### 3.6. Sorption isotherms

To quantify the DC of Zr-SGCS composite, the equations namely Freundlich, Langmuir, and D-R isotherms [11,46–48] have been adopted and the respective equations are given in Table 2.

The Freundlich adsorption isotherm has been interpreted as sorption to heterogeneous surfaces or surface supporting sites of different affinities and can be derived by assuming a logarithmic decrease

Table 2  
Linear forms of isotherms

Isotherms		Linear form	Plot
Langmuir	$q_e = k_F C_e^{1/n}$	$\frac{C_e}{q_e} = \frac{1}{Q^b} + \frac{C_e}{Q}$	$\frac{C_e}{q_e}$ vs. $C_e$
Freundlich	$q_e = \frac{Q^0 b C_e}{1 + b C_e}$	$\log q_e = \log K_F + \frac{1}{n} \log C_e$	$\log q_e$ vs. $\log C_e$
Dubinin–Radushkevich	$q_e = X_m \exp(-k_{DR} \varepsilon^2)$	$\ln q_e = \ln X_m - K_{DR} \varepsilon^2$	$\ln q_e$ vs. $\varepsilon^2$

Table 3  
Freundlich, Langmuir and D–R isotherms of Zr–SGCS composite

Isotherms	Parameters	Temperature		
		303 K	313 K	323 K
Freundlich	$1/n$	0.157	0.183	0.217
	$n$	6.353	5.460	4.612
	$k_F$ (mg/g) (L/mg) $^{1/n}$	4.397	4.435	4.521
	$r$	0.970	0.978	0.982
	SD	0.014	0.013	0.011
	$\chi^2$	0.151	0.202	0.308
Langmuir	$Q^0$ (mg/g)	3.464	3.332	3.170
	$b$ (L/g)	5.693	4.094	3.125
	$R_L$	0.012	0.017	0.022
	$r$	0.999	0.998	0.998
	SD	0.019	0.022	0.023
	$\chi^2$	0.765	0.947	1.087
Dubinin–Radushkevich	$k_{DR}$ (mol $^2$ /J $^2$ )	3.50E–08	4.95E–08	7.08E–08
	$X_m$ (mg/g)	3.837	3.675	3.517
	$E$ (kJ mol $^{-1}$ )	3.780	3.718	2.657
	$r$	0.869	0.907	0.922
	SD	0.065	0.059	0.056
	$\chi^2$	0.389	0.867	0.524

in the enthalpy of sorption with increase in the fraction of occupied sites. Freundlich constants  $K_F$  and  $1/n$  can be determined from the linear plot of  $\log q_e$  vs.  $\log C_e$ . Table 3 implies the values of  $1/n$  lying between 0 and 1 and the  $n$  value lying in the range of 1–10 which confirms the conditions favorable for adsorption [6]. With increase in temperature, the  $k_F$  values were found to increase which indicates that the fluoride removal by Zr–SGCS composite is an endothermic process.

The Langmuir adsorption model is based on monolayer adsorption onto a homogeneous surface and has been successfully applied to model many sorption processes to evaluate the maximum sorption capacity of an adsorbate on an adsorbent. The linear form of Langmuir adsorption isotherm is  $C_e/q_e$  vs.  $C_e$ . The values of  $Q^0$ , Langmuir constant  $b$ , and dimensionless constant  $R_L$  values are given in Table 3. The  $R_L$  values between 0 and 1 indicate favorable adsorption for all the temperatures studied.

The linear form of D–R isotherm was used to determine the type of adsorption for the removal of fluoride from aqueous solution. The values of  $k_{DR}$ ,  $X_m$ ,  $E$ , and  $r$  are shown in Table 3. The obtained  $E$  values in this study lying between 0 and 8 kJ mol $^{-1}$  indicate that the fluoride removal was governed by physisorption [49].

From the above suggested isotherms, the lower  $\chi^2$  values and lower SD values for Freundlich isotherm

as shown in Table 3, confirms its applicability for the sorption process.

### 3.7. Thermodynamic parameters

Thermodynamic parameters provide in-depth information of inherent energetic changes with fluoride sorption; the standard free energy change  $\Delta G^\circ$ , enthalpy change  $\Delta H^\circ$ , and entropy change  $\Delta S^\circ$  were calculated and shown in Table 4.

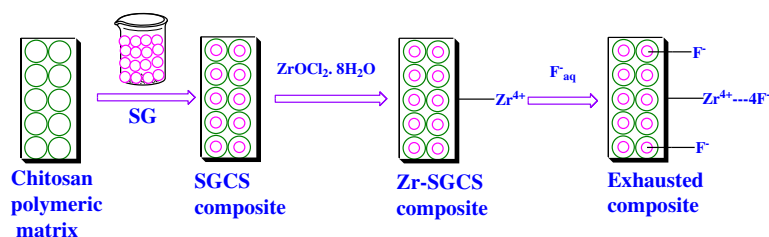
Table 4 shows the values of  $\Delta H^\circ$  and  $\Delta S^\circ$  were obtained from the respective slope and intercept of the Vant Hoff's plot of  $\ln k_0$  against  $1/T$ . The negative  $\Delta G^\circ$  value indicates spontaneous nature of the adsorption process. The value of  $\Delta H^\circ$  for fluoride adsorption is 8.29 kJ mol $^{-1}$ , suggesting that interaction between fluoride and Zr–SGCS composite is endothermic in nature. Further, positive  $\Delta S^\circ$  value indicates the affinity of the adsorbent for fluoride.

Table 4  
Thermodynamic parameters of Zr–SGCS composite

Thermodynamic parameters	Zr–SGCS	
$\Delta G^\circ$ (kJ mol $^{-1}$ )	303 K	–0.44
	313 K	–0.70
	323 K	–1.01
$\Delta H^\circ$ (kJ mol $^{-1}$ )		8.29
$\Delta S^\circ$ (kJ mol $^{-1}$ K $^{-1}$ )		0.03

Table 5  
Kinetic models of Zr-SGCS composite

Kinetic models	Parameters	303 K				313 K				323 K			
		8 mg/L	10 mg/L	12 mg/L	14 mg/L	8 mg/L	10 mg/L	12 mg/L	14 mg/L	8 mg/L	10 mg/L	12 mg/L	14 mg/L
Pseudo-first-order	$k_{ad}$ ( $\text{min}^{-1}$ )	0.007	0.016	0.050	0.065	0.005	0.013	0.015	0.020	0.031	0.015	0.007	0.005
	$r$	0.997	0.991	0.988	0.953	0.964	0.996	0.989	0.965	0.997	0.982	0.987	0.956
Pseudo-second-order	SD	0.005	0.020	0.072	0.186	0.014	0.011	0.021	0.049	0.005	0.014	0.011	0.058
	$q_e$ (mg/g)	3.713	4.383	4.444	5.225	3.423	3.842	4.121	4.532	3.215	3.541	3.875	4.375
	$k$ (g/mg min)	0.0919	0.136	0.230	0.254	0.012	0.071	0.090	0.270	0.05	0.100	0.108	0.118
	$h$ (mg/g min)	0.483	1.236	1.258	1.329	1.058	1.483	1.534	3.368	1.266	1.493	2.619	4.494
	$r$	0.999	0.999	0.999	0.999	0.999	0.999	0.999	0.999	0.997	0.999	0.999	0.999
	SD	0.220	0.076	0.031	0.169	0.116	0.198	0.294	0.115	0.515	0.126	0.255	0.306
Particle diffusion	$k_p$ ( $\text{min}^{-1}$ )	0.045	0.014	0.004	0.008	0.135	0.010	0.007	0.001	0.013	0.006	0.003	0.002
	$r$	0.969	0.990	0.939	0.985	0.972	0.997	0.995	0.983	0.997	0.981	0.990	0.986
Intra particle diffusion	SD	0.242	0.042	0.031	0.030	0.069	0.017	0.015	0.007	0.023	0.027	0.009	0.008
	$k_i$ (mg/g $\text{min}^{0.5}$ )	0.108	0.087	0.062	0.182	0.094	0.110	0.129	0.041	0.171	0.112	0.080	0.091
	$r$	0.992	0.993	0.967	0.987	0.981	0.992	0.999	0.987	0.993	0.992	0.972	0.981
	SD	0.025	0.019	0.030	0.035	0.035	0.025	0.037	0.016	0.039	0.026	0.036	0.034



Scheme 1. Mechanism of fluoride sorption onto Zr-SGCS composite.

Table 6  
Some Zr(IV) based adsorbent for fluoride removal

S. No	Adsorbent	pH	Isotherms	Kinetics	Ref.
1	Zirconium(IV)-propanolamine hybrid material	7	D-R isotherm	Pseudo-second-order	[55]
2	Chitosan supported zirconium(IV) tungstophosphate composite	3	Freundlich	Pseudo-second-order	[56]
3	Zirconium (IV)-metalloporphyrin grafted Fe <sub>3</sub> O <sub>4</sub> nanoparticles	5.5	Not done	Not done	[57]
4	Zirconium-modified-Na-attapulgitite adsorbent	3.7–7.5	Langmuir	Pseudo-second-order	[58]
5	Granular zirconium iron oxide	7	Freundlich	Pseudo-second-order	[59]
6	Hydrous zirconium oxide	4	Freundlich	Pseudo-second-order	[60]
7	Zr(IV) surface-immobilized resin	4–5	Langmuir	Not done	[61]
8	Meso-structured zirconium phosphate	6	D-R isotherm	Pseudo-second-order	[62]
9	Zirconium impregnated cashew nut shell carbon	7	Langmuir	Pseudo-second-order	[63]
10	Zirconium (IV) doped chitosan bio-composite	6–6.9	Freundlich	Not done	[43]
11	Zr(IV)-ethylenediamine	7	D–R isotherm	Pseudo-second-order	[64]
12	Zirconium(IV)-impregnated collagen fiber	<5	Langmuir	Pseudo-first-order	[65]
13	Zr(IV) entrapped chitosan polymeric matrix	7	Freundlich	Not done	[66]
14	Zr-loaded garlic peel (Zr-GP) particles	4	Langmuir	Pseudo-second-order	[67]
15	Hydrous iron(III)-zirconium(IV) hybrid oxide	4.0–7.0	Redlich–Peterson	Pseudo-first-order and reversible-first-order	[68]
16	Alginate entrapped Fe(III)-Zr(IV) binary mixed oxide	6	Langmuir	Pseudo-second order	[69]
17	Zr(IV) entrapped SGCS composite	7	Freundlich	Pseudo-second order	Present study

### 3.8. Sorption dynamics

#### 3.8.1. Reaction-based model

To investigate the rate of the sorption of fluoride onto Zr-SGCS composite, the most popular linear forms of pseudo-first-order [50] and pseudo-second-order [51] kinetic models had been used at different experimental conditions.

The coefficient of determination,  $r^2$  was calculated for both linear and nonlinear methods of the pseudo-second-order model and is presented in Table 5 along with experimental data for  $q_e$ ,  $k$ , and  $h$ . As shown in Table 5, higher  $r^2$  values obtained by the nonlinear method indicate the greater applicability of the nonlinear pseudo-second-order model than of the linear model.

### 3.8.2. Diffusion-based model

For a solid–liquid sorption process, the solute transfer is usually characterized either by particle diffusion or by intraparticle diffusion control [52,53]. The equations for both the diffusion model values of  $k_p$ ,  $k_i$ , and  $r$  are presented in Table 5, and the higher  $r$  values in both the cases indicated the possibility of sorption process being controlled by both the particle and intraparticle diffusion models.

Among the diffusion-based models, the intraparticle diffusion model was found to have less  $r$  values indicates that the sorbent removes fluoride by intraparticle diffusion rather than particle diffusion.

## 4. Mechanism for fluoride removal

The electrostatic interaction exists between silica ( $\text{Si-O}^-$ ) and chitosan ( $\text{NH}_3^+$ ) as reported by Lai et al. [54], holds them together. The mechanism of fluoride removal of Zr–SGCS composite was mainly governed by adsorption and is illustrated in Scheme 1. During the entrapping of Zr(IV) from  $\text{ZrOCl}_2 \cdot 8\text{H}_2\text{O}$  into the SGCS composite the amino group of chitosan have chelated with  $\text{Zr}^{4+}$ . The positively charged  $\text{Zr}^{4+}$  surface in the Zr–SGCS composite and the free amine groups of chitosan attracts the negatively charged fluoride by means of electrostatic attraction. The fluoride removal by SG is mainly due to its porous nature which entraps fluoride. Hence, an enhancement in  $q$  value of Zr–SGCS composite over SGCS composite may be due to the presence of porosity and higher charge of  $\text{Zr}^{4+}$  which strongly adsorb fluoride.

A comparison has been made between Zr–SGCS composite and previously reported zirconium-based adsorbents [55–69] for fluoride removal and is presented in Table 6.

## 5. Conclusions

In this study, Zr–SGCS composite was prepared and its fluoride adsorption capacity was evaluated. The following conclusions were drawn from the above studies.

- The fluoride adsorption was practically achieved with maximum DC of 4,530  $\text{mgF}^-/\text{kg}$  at 60 min.
- The maximum removal of  $\text{F}^-$  was observed at pH 7.
- The best-fitting adsorption isotherm was found to be Freundlich isotherm model.
- The adsorption process was spontaneous and endothermic in nature.
- Kinetic data were fitted to pseudo-second-order model and intraparticle diffusion model.

- The Zr(IV)-chelated by amino groups in chitosan electrostatically adsorb fluoride.
- From this study, it has been concluded that Zr–SGCS could be an alternative promising sorbent for fluoride removal from aqueous solution.

## Acknowledgment

Authors are grateful to the UGC-Research fellowship for sciences to meritorious students (RFSMS) for the financial support to carry out this research work.

## References

- [1] M. Amini, K. Mueller, K.C. Abbaspour, T. Rosenberg, M. Afyuni, K.N. Møller, M. Sarr, C.A. Johnson, Statistical modeling of global geogenic fluoride contamination in ground waters, *Environ. Sci. Technol.* 42 (2008) 3662–3668.
- [2] WHO Report, Fluoride and Fluorides: Environmental Health Criteria, World Health Organisation, Geneva, 1984.
- [3] M. Srimurali, J. Karthikeyan, Activated alumina: Defluoridation of water and household application—A study, Twelfth International Water Technology Conference, IWTC12, Alexandria, Egypt, 2008.
- [4] C.J. Huang, J.C. Liu, Precipitate flotation of fluoride-containing wastewater from a semiconductor manufacturer, *Water Res.* 33 (1999) 3403–3412.
- [5] K.M. Popat, P.S. Anand, B.D. Dasare, Selective removal of fluoride ion from water by the aluminium form of the aminomethylphosphonic acid type ion exchanger, *React. Polym.* 23 (1994) 23–32.
- [6] S. Meenakshi, N. Viswanathan, Identification of selective ion exchange resin for fluoride sorption, *J. Colloid Interface Sci.* 308 (2007) 438–450.
- [7] S.V. Joshi, S.H. Mehta, A.P. Rao, A.V. Rao, Estimation of sodium fluoride using HPCL in reverse osmosis experiments, *Water Treat.* 7 (1992) 207–211.
- [8] R. Simons, Trace element removal from ash dam waters by nanofiltration and diffusion dialysis, *Desalination* 89 (1993) 325–341.
- [9] S.K. Adhikary, U.K. Tipnis, W.P. Harkare, K.P. Govindan, Defluoridation during desalination of brackish water by electrodialysis, *Desalination* 71 (1989) 301–312.
- [10] M. Hichour, F. Persin, J. Sandeaux, C. Gavach, Fluoride removal from waters by donnan dialysis, *Sep. Purif. Technol.* 18 (2000) 1–11.
- [11] S. Kundu, A.K. Gupta, Arsenic adsorption onto iron oxide coated cement (IOCC): Regression analysis of equilibrium data with several isotherm models and their optimization, *Chem. Eng. J.* 122 (2006) 93–106.
- [12] M.S. Onyango, D. Kuchar, M. Kubota, H. Matsuda, Adsorptive removal of phosphate ions from aqueous solution using synthetic zeolite, *Ind. Eng. Chem. Res.* 46 (2007) 894–900.
- [13] K.K.H. Choy, J.F. Porter, G. McKay, Film—Pore diffusion models—Analytical and numerical solutions, *Chem. Eng. Sci.* 59 (2004) 501–512.

- [14] Meenakshi, R.C. Maheshwari, Fluoride in drinking water and its removal, *J. Hazard. Mater.* 137 (2006) 456–463.
- [15] L. Jin, R. Bai, Mechanisms of lead adsorption on chitosan/PVA hydrogel beads, *Langmuir* 18 (2002) 9765–9770.
- [16] W. Ma, F.Q. Ya, M. Han, R. Wang, Characteristics of equilibrium, kinetics studies for adsorption of fluoride on magnetic-chitosan particle, *J. Hazard. Mater.* 143 (2007) 296–302.
- [17] N. Viswanathan, C. Sairam Sundaram, S. Meenakshi, Removal of fluoride from aqueous solution using protonated chitosan beads, *J. Hazard. Mater.* 161 (2009) 443–450.
- [18] N. Viswanathan, S. Meenakshi, Selective sorption of fluoride using Fe(III) loaded carboxylated chitosan beads, *J. Fluorine Chem.* 129 (2008) 503–509.
- [19] N. Viswanathan, S. Meenakshi, Enhanced fluoride sorption using La(III) incorporated carboxylated chitosan beads, *J. Colloid Interface Sci.* 322 (2008) 375–383.
- [20] R.A.A. Muzzarelli, *Natural Chelating Polymers: Alginic Acid, Chitin and Chitosan*, Pergamon Press, New York, NY, 1973.
- [21] J. Retuert, R. Quijada, V. Arias, M.Y. Pedram, Porous silica derived from chitosan-containing hybrid composites, *J. Mater. Res.* 18 (2003) 487–494.
- [22] S.B. Park, J.O. You, H.Y. Park, S.J. Haam, W.S. Kim, A novel pH-sensitive membrane from chitosan—TEOS IPN: Preparation and its drug permeation characteristics, *Biomaterials* 22 (2001) 323–330.
- [23] F. Li, P. Du, W. Chen, S. Zhang, Preparation of silica-supported porous sorbent for heavy metal ions removal in wastewater treatment by organic-inorganic hybridization combined with sucrose and polyethylene glycol imprinting, *Anal. Chem. Acta* 585 (2007) 211–218.
- [24] F. Li, H. Jiang, S. Zhang, An ion-imprinted silica-supported organic-inorganic hybrid sorbent prepared by a surface imprinting technique combined with a polysaccharide incorporated sol-gel process for selective separation of cadmium(II) from aqueous solution, *Talanta* 71 (2007) 1487–1493.
- [25] S.M.C. Ritchie, L.G. Bachas, T. Olin, S.K. Sikdar, D. Bhattacharyya, Surface modification of silica and cellulose-based microfiltration membranes with functional polyamino acids for heavy metal sorption, *Langmuir* 15 (1999) 6346–6357.
- [26] A.D. Ebner, J.A. Ritter, J.D. Navratil, Adsorption of cesium, strontium and cobalt ions on magnetite and magnetite-silica composite, *Ind. Eng. Chem. Res.* 40 (2001) 1615–1623.
- [27] K. Molvinger, F. Quignard, D. Brunel, M. Boissiere, J.M. Devoisselle, Porous chitosan-silica hybrid microspheres as potential catalyst, *Chem. Mater.* 16 (2004) 3367–3372.
- [28] Y. Miao, S.N. Tan, Amperometric hydrogen peroxide biosensor with silica sol-gel/chitosan film as immobilization matrix, *Anal. Chim. Acta* 437 (2001) 87–93.
- [29] M. Kato, H. Saruwatari, K. Sakai-Kato, T. Toyō'oka, Silica sol-gel/organic hybrid material for protein encapsulated column of capillary electrochromatography, *J. Chromatogr. A* 2004 (1044) 267–270.
- [30] Y. Wang-zhang, P. Mao, Y. Qiu-ming, T. Ben-zhong, Z. Qiang, Synthesis and characterization of polystyrene/nanosilica organic-inorganic hybrid, *Chem. Res. Chin. Univ.* 22 (2006) 797.
- [31] M. Rajiv Gandhi, S. Meenakshi, Preparation and characterization of silica gel/chitosan composite for the removal of Cu(II) and Pb(II), *Int. J. Biol. Macromol.* 50 (2012) 650–657.
- [32] J.E. Harwood, D.J. Huyser, The automated analysis of fluoride in water using zirconium-xylene orange, *Water Res.* 2 (1968) 637–642.
- [33] D. Chen, M.D.L. de Castro, M. Valcárcel, Fluorimetric sensor for the determination of fluoride at the nanograms per millilitre level, *Anal. Chim. Acta* 234 (1990) 345–352.
- [34] APHA, *Standard Methods for the Examination of Water and Waste Water*, American Public Health Association, Washington, DC, 2005.
- [35] M.V. Lopez-Ramon, F. Stoeckli, C. Moreno-Castilla, F. Carrasco-Marin, On the characterization of acidic and basic surface sites on carbons by various techniques, *Carbon* 37 (1999) 1215–1221.
- [36] M. Rajiv Gandhi, S. Meenakshi, Preparation and characterization of La(III) encapsulated silica gel/chitosan composite and its metal uptake studies, *J. Hazard. Mater.* 203–204 (2012) 29–37.
- [37] S.H. Park, S. McClain, Z.R. Tian, S.L. Suib, C. Karwacki, Surface and bulk measurements of metals deposited on activated carbon, *Chem. Mater.* 9 (1997) 176–183.
- [38] J.P. Chen, S.N. Wu, Acid/base-treated activated carbons: Characterization of functional groups and metal adsorptive properties, *Langmuir* 20 (2004) 2233–2242.
- [39] L.J. Kennedy, J.J. Vijaya, G. Sekaran, K. Kayalvizhi, Equilibrium, kinetic and thermodynamic studies on the adsorption of m-cresol onto micro- and mesoporous carbon, *J. Hazard. Mater.* 149 (2007) 134–143.
- [40] D.M. Pickup, G. Mountjoy, G.W. Wallidge, R.J. Newport, M.E. Smith, Structure of  $(ZrO_2)_x(SiO_2)_{1-x}$  xerogels ( $x=0.1, 0.2, 0.3$  and  $0.4$ ) from FTIR,  $^{29}Si$  and  $^{17}O$  MAS, NMR and EXAFS, *Phys. Chem. Chem. Phys.* 1 (1999) 2527–2533.
- [41] S.G. Chen, Y.S. Yin, Formation of ring-like Si–O–Zr bonds at intergranular interfaces in silica-doped zirconia, *J. Am. Ceram. Soc.* 88 (2005) 1041–1045.
- [42] N. Kazuo, *Infrared and Raman Spectra of Inorganic and Coordination Compound*, Wiley, New York, NY, 1978.
- [43] R. Dongre, D.N. Ghugal, J.S. Meshram, D.S. Ramteke, Fluoride removal from water by zirconium (IV) doped chitosan bio-composite, *Afr. J. Environ. Sci. Technol.* 6 (2012) 130–141.
- [44] Y.K. Nakano, K. Takeshita, T. Tsutsumi, Adsorption mechanism of hexavalent chromium by redox within condensed-tanning gel, *Water Res.* 35 (2001) 496–500.
- [45] D. Zhou, L. Zhang, S. Guo, Mechanisms of lead biosorption on cellulose/chitin beads, *Water Res.* 39 (2005) 3755–3762.
- [46] H.M.F. Freundlich, Über die adsorption in lösungen, *Z. Phys. Chem.* 57A (1906) 385–470.
- [47] I. Langmuir, The constitution and fundamental properties of solids and liquids, *J. Am. Chem. Soc.* 38 (1916) 2221–2295.
- [48] S. Karahan, M. Yurdakoç, Y. Seki, K. Yurdakoç, Removal of boron from aqueous solution by clays

- and modified clays, *J. Colloid Interface Sci.* 293 (2006) 36–42.
- [49] E. Eren, Removal of basic dye by modified unye bentonite, Turkey, *J. Hazard. Mater.* 162 (2009) 1355–1363.
- [50] S. Lagergren, Zur theorie der sogenannten adsorption gelöster stoffe, *K. Sven. Vetenskapsakad. Handl.* 24 (1898) 1–39.
- [51] Y.S. Ho, Second order kinetic model for the sorption of cadmium onto tree fern: A comparison of linear and non linear methods, *Water Res.* 40 (2006) 119–125.
- [52] M. Chanda, K.F. O'Driscoll, G.L. Rempel, sorption of phenolics onto cross-linked poly(4-vinyl pyridine), *React. Polym.* 1 (1983) 281–293.
- [53] W.J. Weber, J.C. Morris, Equilibria and capacities for adsorption on carbon, *J. Sanitary Eng. Div.* 90 (1964) 79–91.
- [54] S.M. Lai, A.J.M. Yang, W.C. Chen, J.F. Hsiao, The properties and preparation of chitosan/silica hybrids using sol-gel process, *Polym. Plast. Technol. Eng.* 45 (2006) 997–1003.
- [55] S.K. Swain, S. Mishra, P. Sharma, T. Patnaik, V.K. Singh, U. Jha, R.K. Patel, R.K. Dey, Development of a new inorganic-organic hybrid ion-exchanger of zirconium(IV)-propanolamine for efficient removal of fluoride from drinking water, *Ind. Eng. Chem. Res.* 49 (2010) 9846–9856.
- [56] N. Viswanathan, S. Meenakshi, Development of chitosan supported zirconium(IV) tungstophosphate composite for fluoride removal, *J. Hazard. Mater.* 176 (2010) 459–465.
- [57] T. Poursaberi, M. Hassanisadi, K. Torkestani, M. Zare, Development of zirconium (IV)-metalloporphyrin grafted Fe<sub>3</sub>O<sub>4</sub> nanoparticles for efficient fluoride removal, *Chem. Eng. J.* 189–190 (2012) 117–125.
- [58] G. Zhanga, Z. Hea, W. Xub, A low-cost and high efficient zirconium-modified-Na-attapulgit adsorbent for fluoride removal from aqueous solutions, *Chem. Eng. J.* 183 (2012) 315–324.
- [59] X. Dou, Y. Zhang, H. Wang, T. Wang, Y. Wang, Performance of granular zirconium-iron oxide in the removal of fluoride from drinking water, *Water Res.* 45 (2011) 3571–3578.
- [60] X. Dou, D. Mohan, C.U.P. Jr, S. Yang, Remediating fluoride from water using hydrous zirconium oxide, *Chem. Eng. J.* 198–199 (2012) 236–245.
- [61] S. Samatya, H. Mizuki, Y. Ito, H. Kawakita, K. Uezu, The effect of polystyrene as a porogen on the fluoride ion adsorption of Zr(IV) surface-immobilized resin, *React. Funct. Polym.* 70 (2010) 63–68.
- [62] S.K. Swain, T. Patnaik, V.K. Singh, U. Jha, R.K. Patel, R.K. Dey, Kinetics, equilibrium and thermodynamic aspects of removal of fluoride from drinking water using meso-structured zirconium phosphate, *Chem. Eng. J.* 171 (2011) 1218–1226.
- [63] G. Alagumuthu, M. Rajan, Equilibrium and kinetics of adsorption of fluoride onto zirconium impregnated cashew nut shell carbon, *Chem. Eng. J.* 158 (2010) 451–457.
- [64] S.K. Swain, S. Mishra, T. Patnaik, R.K. Pateld, U. Jha, R.K. Dey, Fluoride removal performance of a new hybrid sorbent of Zr(IV)-ethylenediamine, *Chem. Eng. J.* 184 (2012) 72–81.
- [65] X.P. Liao, B. Shi, Adsorption of fluoride on zirconium (IV)-impregnated collagen fiber, *Environ. Sci. Technol.* 39 (2005) 4628–4632.
- [66] N. Viswanathan, S. Meenakshi, Synthesis of Zr(IV) entrapped chitosan polymeric matrix for selective fluoride sorption, *J. Colloid Interface Sci.* 72 (2009) 88–93.
- [67] H. Kai, S. Jiu-gang, Z. Hong-min, I. Katsutoshi, Removal of fluoride from aqueous solution onto Zr-loaded garlic peel (Zr-GP) particles, *J. Cent. South Univ. Technol.* 18 (2011) 1448–1453.
- [68] K. Biswas, D. Bandhoyapadhyay, U.C. Ghosh, Adsorption kinetics of fluoride on iron(III)-zirconium (IV) hybrid oxide, *Adsorption* 13 (2007) 83–94.
- [69] S.K. Swain, T. Patnaik, P.C. Patnaik, U. Jha, R.K. Dey, Development of new alginate entrapped Fe(III)-Zr(IV) binary mixed oxide for removal of fluoride from water bodies, *Chem. Eng. J.* 215–216 (2013) 763–771.